

Chain trajectory in solution grown polyethylene crystals: correlation between infra-red spectroscopy and small-angle neutron scattering

S. J. Spells, D. M. Sadler and A. Keller

H. H. Wills Physics Laboratory, University of Bristol, Royal Fort, Tyndall Avenue, Bristol BS8 1TL, UK

(Received 28 June 1979; revised 12 March 1980)

Infra-red (i.r.) measurements of the CD₂ bending vibration have been made for polyethylene single crystals of mixed isotopic composition under a wider range of conditions than hitherto. A comparison with data for mixed paraffin crystals shows that the polymer molecules exist in a compact conformation, consistent with the 'superfolded' structure which has emerged from small angle neutron scattering (SANS) measurements. However, the correlation splitting of the CD₂ bending vibration, a prominent feature of previous studies, is not generally observed. At 'guest' concentrations of 1%, SANS data indicate minimal isotopic fractionation, and it is only at such low concentrations that the band-shape of the CD₂ bending vibration primarily reflects intra-chain effects due to chain conformation. Previous SANS data at wider angles ($10^{-1} > s > 10^{-2} \text{ \AA}^{-1}$) lead to an estimate of about 0.5 for the fraction of stem sites along a folded ribbon occupied by a single molecule. A study of the i.r. peak broadening leads to a similar value for the local concentration.

INTRODUCTION

The organization of polymer chains within lamellar crystals has been a long-standing issue and is attracting renewed interest with the advent of small angle neutron scattering (SANS) studies of isotopically mixed systems¹⁻⁴. The main purpose of the present paper is to attempt a correlation between these recent neutron scattering results and related infra-red work (i.r.) reported previously⁵⁻⁹. It will be seen that the two methods applied to identical samples will prove to be complementary. Although relying on different physical principles, the inferences reached from one will assist in the interpretation of the other. First, however, the present status of the two lines of research, to be brought together in the present paper, will be recapitulated insofar as is necessary for the appreciation of the new objectives and attainments.

The common feature of both lines of research has been the employment of isotopic doping. In particular, the usual hydrogenated polyethylene (PEH) is doped with deuterated polyethylene (PED or *vice versa*, the two species being crystallized together*. If it is assumed that the crystallization itself is unaffected by the isotopic nature of the chain, the organization of an isolated chain within its own crystalline environment can then be explored by methods sensitive to the isotopic labelling. The two methods (i.r. and SANS) achieve this purpose in different ways, to be reviewed briefly below.

* It emerged that at high supercoolings, the two isotopic species co-crystallize sufficiently randomly for these experiments; on slow crystallization at low supercoolings segregation or enrichment of the two species in different crystal zones can occur^{2,4}.

I.r. method

This was the first of the techniques to utilize the potential of isotopic doping, to the credit of Krimm and coworkers⁵⁻⁹. It relies on the fact that certain i.r. bands are doublets: the orthorhombic unit cell of polyethylene contains two chains which are not symmetrically equivalent, and hence both in-phase and out-of-phase vibrations are observed. Such correlation splittings, however, are only expected when the interacting chains are isotopically identical, the appropriate doublets being situated at different frequencies for PEH and PED. If one of the isotopic species is present in high dilution ('guest' molecule), chance contact between different guest molecules will be much reduced compared with the pure species. Splitting of the appropriate band associated with the guest species will then only arise if (a) segments from the same molecule are in contact, and if (b) such adjacent chain portions are crystallographically non-equivalent. Condition (a) requires the presence of adjacent fold stems: this is a necessary requirement for adjacent fold re-entry in a chain folded crystal, but would not necessarily be compelling evidence for such a scheme of folding. Condition (b) specifically requires a {110} fold plane. Krimm has calculated the amount of splitting for a {110} fold plane as a function of the concentration of guest molecules, taking the guest fold planes to be of infinite extent¹⁰. The planes of different isotopic composition are assumed to stack in a regular pattern. It will be evident that the experimental method should provide information on the two cardinal issues adjacency of folding and the direction of the fold plane.

The conclusions reported by Krimm and coworkers are as follows. The guest splitting, amounting to several

wavenumbers in peak separation, is always present in solution grown crystals, demonstrating the validity of the model of adjacent re-entry. The magnitude of the splitting is, moreover, in quantitative agreement with predictions for highly extended $\{110\}$ fold planes¹⁰. (The results were checked against paraffins which only display splitting at high guest concentrations in agreement with expectations from random mixing of individual straight chains⁵. However, no guest splitting was observed in melt crystallized samples⁵, or in single crystals refolded on heat annealing⁹. Yet even in these cases *small* differences (1 cm^{-1} or less) were seen in the splittings of bands associated with the *host* molecules in comparison with expected values for a system with guest stems randomly mixed within the host matrix. These small changes may be compared with a value of about 10.5 cm^{-1} for the splitting in PEH. It was concluded that adjacently re-entrant folding is still present in these cases, but that the folds connect crystallographically equivalent chains, so that no guest splitting is observed. Folding along *b*, $\{100\}$ fold plane, was found to satisfy this criterion. Note that the case for adjacent re-entry in melt grown crystals relies on a much smaller and subtler effect than that for solution grown crystals where the doublet (as opposed to the singlet) nature of the appropriate guest band should in itself provide qualitative evidence for adjacent stems in the $\{110\}$ plane.

SANS method

This method relies on the difference in neutron scattering amplitude between the two isotopic species. It follows that the neutrons will be scattered by the low concentration guest species as if by isolated chains. The experiments fall within two angular scattering ranges.

Medium angle range $10^{-1} > s > 10^{-2} \text{ \AA}^{-1}$ where $s = 2 \sin \theta / \lambda$, 2θ being the scattering angle and λ the wavelength. Information obtainable from this range relates to the details of the molecular trajectory. Thus it was possible to establish that in solution grown crystals the angular dependence of the intensity is accountable by sheet shaped entities, each molecule probably occupying several such objects. For low molecular weight, the sheets are compatible with single layers of adjacent stems belonging to the same chain (thus implying adjacent fold re-entry). For high molecular weight multiple layers were invoked^{1,2}. These findings are in sharp contrast with the functional relations observed between intensity and scattering angle in melt crystallized samples. In samples prepared by fairly rapid cooling (the only ones amenable to such experiments — see footnote above), the asymptotic behaviour of the intensity was consistent with rod shaped entities scattering independently, this being related to separate fold stems (implying re-entry which is random to some degree)². The dimensions involved (i.e. thickness of the sheets, or diameter of the rods) were compared with molecular dimensions, as calculated from the cross-sections of the chains. Similarly the derived isotope densities in the scattering entity (number of deuterium atoms per unit length of rod for rod scatterers and the number per unit lamellar area for sheets) were also compared with expectations. The dimensions and isotope densities were in good agreement for the independent rods (melt growth). The values for sheet thicknesses (solution growth) were consistent with those for single sheets

although a molecular weight dependence was observed, indicating increased sheet thicknesses for higher molecular weights. Isotope occupation densities also varied with molecular weight but were always about half those expected. Nevertheless, irrespective of the departures mentioned, as a first stage the correspondence with the idealized sheet model incorporating adjacent re-entry and with the random re-entry rod model in the respective cases was considered satisfactory. The small value of deuterium density per unit area for solution grown crystals acquires significance in the present work.

Low angles, $s < 10^{-2} \text{ \AA}^{-1}$. Radii of gyration R_g , obtainable for this range of s , were the first results obtained with the SANS technique on amorphous and liquid polymers³. These showed that R_g was the same as for a theta solvent, and the expected $M_w^{1/2}$ dependence was found (M_w is the weight-average molecular weight). For crystalline polyethylene it was found necessary to compare the absolute value of the forward scattering (i.e. the limiting value of intensity as 2θ goes to zero) with that predicted from the known molecular weight. In many cases an additional contribution to the intensity is present, which means that the total intensity cannot be simply related to the scattering of individual tagged molecules for all values of s . It is clear that the guest molecules are not always distributed randomly. Detailed examination has shown that the guest molecules do not 'cluster'⁴ but that long range fluctuations in guest concentrations occur as a result of differences in crystallization rate (fractionation)^{2,11}. As a consequence of the long range of these fluctuations, for many experiments it is possible to identify the forward scattering from individual molecules (e.g. for a region of s around $3 \times 10^{-3} \text{ \AA}^{-1}$). In general the 'fractionation signal' is only of any consequence in the region of low s since it decreases rapidly with increasing s (approximately as s^{-4}). This limits the range of samples for which R_g values are measurable, a necessary condition in general being the use of high supercoolings (see the previous footnote). While the fractionation signal is an inconvenience, it does give useful information for the interpretation of the i.r. effects.

Both the absolute value of R_g and its molecular weight dependence were found to be retained on fast crystallization from the melt⁴. This shows that the conformation of the chain on a large scale is retained. On crystallization from solution, however, R_g proved to be smaller than its theta-solvent value². More recent work extended the R_g determination on solution crystallized material to include a systematic study of its variation with molecular weight¹². This has led to unexpected behaviour: R_g proved to be largely independent of molecular weight (*Figure 1*), in sharp contrast to what is observed in the melt (also shown in *Figure 1*). R_g was found to vary as $R_g \propto M_w^{0.1}$. As explained in ref. 12, this striking observation can be accounted for if a chain folded ribbon itself folds up beyond a certain length, as the resulting increase in the ribbon thickness would hardly affect the radius of gyration, in spite of an appreciable increase in mass. The molecular weight at which the single fold ribbon folds back on itself is shown by the above evidence to be in the range of 50 000. This new structural concept we termed 'superfolding'. Note that this phenomenon is consistent with the increase in sheet thickness with molecular weight inferred from scattering at medium angles (range (a)

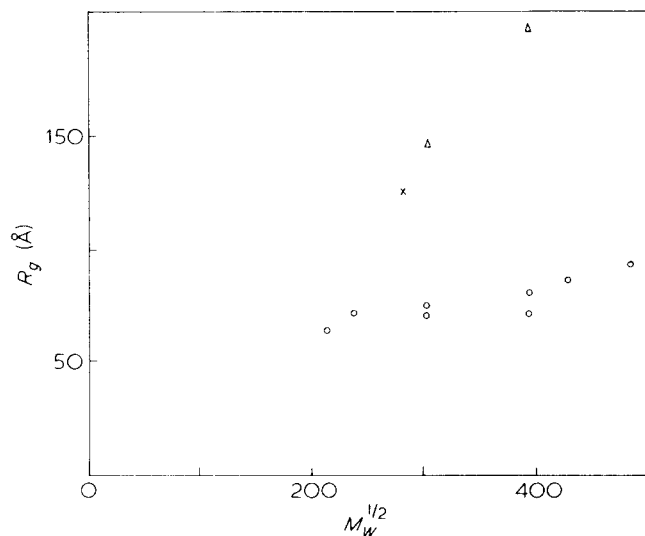


Figure 1 Equivalent radii of gyration (R_g) derived from data of the type shown in Fig. 3 of ref. 12. Details of sample preparation and background corrections are described there. In all cases the PED concentration is 1%. Since the Zimm formulation of the low angle scattering describes the data to larger s than does the Guinier formulation², the R_g were derived from least squares fits of inverse intensity versus s^2

above) in requiring multiple sheets. Furthermore, the stacking of these sheets need not be strictly adjacent. It also fits into existing notions of crystallization kinetics, as its onset would correspond to the transition from regime I to regime II crystallization¹³, a behaviour which, while explored quantitatively in melt crystallization, was nevertheless foreshadowed in a qualitative manner in discussions on solution grown crystals¹⁴.

Objectives

The need for correlating i.r. and SANS measurements, preferably on identical samples, is self-evident. For solution grown crystals interpretations agree, but not for melt grown crystals. (In the latter case, adjacent folding is suggested by i.r., but random folding by SANS.) We state at the outset that the present work did not progress beyond solution grown crystals, because we encountered an unexpected situation, namely that we could only observe the anticipated i.r. band splitting for a restricted range of conditions (high molecular weight and relatively high guest concentrations). This we set out to explore in the rest of the work by an approach which has remained purely empirical, using peak widths as a measure of guest chain interactions.

EXPERIMENTAL

Sample preparation

Mixed crystal mats of polyethylene were prepared from xylene solution as previously described², a crystallization temperature of 70°C being used in most cases, apart from a few samples crystallized at 85°C. In addition, several mats were quenched from the melt into an ice-water mixture. Enhanced fractionation of isotopic species, to be used for some of the experiments, was achieved in the following manner: first, PEH was crystallized from xylene using thin-walled glass tubes immersed in an oil bath which was held at 70°C. A solution of PED in xylene was then added, and the PED was allowed to crystallize in the

usual way. By this method, samples with a range of overall PED concentrations from 0.3 to 10% were obtained.

Mixed crystals of dotriacontane ($C_{32}X_{66}$; X = H or D) were also used for i.r. measurements. Samples were obtained in two ways: evaporation of solvent from a solution of the paraffins in benzene at room temperature was followed by pressing to produce a self-supporting mat. For a thinner specimen, the sample was cast directly from hot benzene solution onto a KBr plate.

Infra-red spectroscopic measurements

Most i.r. measurements were made on the 1085/1092 cm^{-1} CD_2 bending doublet, but measurements are also reported here on the 1462/1473 cm^{-1} CH_2 bending vibration and the CD_2 rocking doublet at 519/526 cm^{-1} . Spectra were recorded using a Perkin Elmer 225 IR spectrometer, using a spectral bandwidth of between 0.7 and 1.5 cm^{-1} and scanning speeds of 2–3 cm^{-1}/min . A weak absorption band at about 1080 cm^{-1} in the i.r. spectrum of PEH, previously assigned to a carbon-carbon stretching vibration¹⁵, gave rise to problems in background subtraction with PED concentrations as low as 1%. To overcome these problems a PEH reference sample, prepared under the same conditions as the mixed crystal mat in the sample beam, was placed in the reference beam. The PEH reference was chosen to match the thickness of the PED/PEH sample to within about 10%, so that the signal obtained was principally the absorption of the 1085/1092 cm^{-1} CD_2 bending doublet.

Neutron scattering measurements

Measurements were made on the D11 low angle facility at the Institut Laue Langevin (Grenoble)¹⁶. Spectra were recorded for approximately 70–100 mg of material (10 mm × 10 mm in area) of the sample blend and also for a purely hydrogenous 'background' sample and for the sample holder only. The corrected net intensity is the difference between the sample signal and that for the same weight of background, slight corrections being necessary to allow for the variations of about 10% in the weights of different specimens. A scaling operation was carried out in order to allow for variations in counter response with 2θ , using a spectrum from H_2O as a calibration specimen. The calibration was performed by using measurements of incoherent scattering, together with the measured transmission of the main beam^{2,17}.

RESULTS

Infra-red spectroscopy

The examinations were centred on the CD_2 bending vibration of the 'guest' species. The sample types used were as follows:

- (1) Mixed crystals of paraffins in the concentration range of 3–100% perdeuterated dotriacontane (PDD).
- (2) Mixed crystals of polyethylenes in the concentration range of 1–5% PED prepared by: (a) crystallization from solution at 70°C for PED molecular weights from 45 000 to 386 000 (M_w); (b) quenching from the melts for two samples with PED molecular weights of 81 000 and 155 000; (c) Consecutive crystallization of PEH and PED from solution at 70°C to achieve artificial enhancement of isotopic

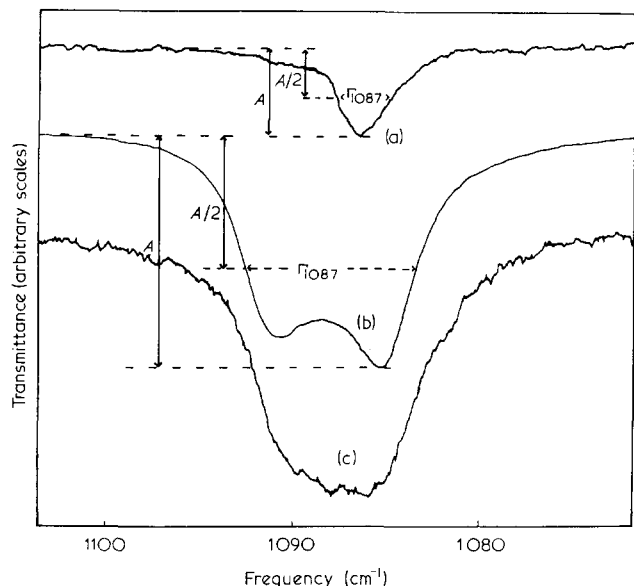


Figure 2 Infra-red spectra of the CD_2 bending region. (a) Mixed $\text{C}_{32}\text{H}_{66}/\text{C}_{32}\text{D}_{66}$ mat with 3% PDD; (b) mixed polyethylene mat crystallized at 70°C with 5.4% PED of M_w 386 000; (c) mixed polyethylene mat crystallized at 70°C with 3% PED of M_w 386 000. Also shown schematically is the method of defining the measured bandwidth (Γ_{1087}) in terms of the peak absorbance (A)

fractionation. The PED had a molecular weight of 207 000.

As indicated in the Introduction, splitting of the bending vibration for the guest species was not in general observed. The conditions found necessary for the doublet to be resolved may be summarized as follows:

- (1) In mixed paraffin crystals, a PDD concentration greater than about 55% is required.
- (2) For mixed polyethylene crystals grown at high supercoolings from solution a PED concentration of at least 5% and a molecular weight of at least 234 000 are required.
- (3) In mixed polyethylene crystals with enhanced isotopic fractionation, splittings can be observed with a guest concentration of 3%.

The CD_2 doublet was *not* resolved in the following circumstances: (1) for mixed polyethylene crystals grown at high supercoolings from solution with molecular weights up to 386 000 and PED concentrations of 1 and 3%; (2) for the mixed polyethylene crystals quenched from the melt.

Even though the expected band splittings were not generally observed, the band widths (Γ) for solution grown crystals approach those of a doublet. Figures 2 (b) and (c) show guest bands with and without splitting, and 2(a) shows for comparison a singlet guest band in a mixed paraffin sample.

The Figure also shows how the broadening parameter Γ (full peak width at half maximum absorbance) was defined. It is reasonable to assume that the broadening of a guest singlet, without the appearance of correlation splitting, is the result of guest chain interactions which are extensive, but not sufficiently so for the development of a doublet. Hence, systematic measurements of Γ should provide a means of investigating interactions between CD_2 groups in neighbouring chains. In addition to showing Γ values, we indicate when the doublet is resolved. The information obtained from Γ values is

analogous to that derived from measurements of resolved doublet splittings.

Paraffin mixtures were studied in order to measure both the effects of chain interaction on Γ and the development of correlation splitting in situations where the guest stems have a disordered arrangement. i.e. measurements for mixed paraffin mats with PDD concentrations of between 3% and 100% are shown in Figure 3. The CD_2 bending doublet was resolved for PDD concentrations greater than about 55%. The relationship between Γ and PDD concentration is approximately linear.

In Figure 4 Γ is plotted against PED concentration for solution grown polyethylene mixed crystal mats, for guest PED of M_w 386 000 and approximately 100 000. It can be seen that within the errors involved, Γ generally increases with both increasing PED molecular weight and concentration. The CD_2 bending doublet was only resolved for the sample with 5% PED of M_w 386 000. Nevertheless, at this molecular weight a much lower concentration of the deuterated species is required for the splitting to be resolved than is the case for mixed paraffin samples (Figure 3).

In Figure 5 Γ is plotted against M_w for solution-grown and melt-quenched mixed polyethylene crystals with 1% PED. The value of Γ for mixed paraffin crystals with 3% PDD is also shown for comparison. Γ increases somewhat with PED molecular weight for solution grown mixed polyethylene samples and the bandwidths observed are significantly greater than for samples quenched from the melt.

The degree of isotopic fractionation in various samples, as measured by SANS, is discussed in the following section. We simply note here that an increase in Γ has been observed in cases where the degree of fractionation was increased either by (i) consecutive crystallization of PEH and PED (samples 2 (c) above) or (ii) crystallization at the higher temperature of 85°C .

It is noted that the CD_2 rocking doublet, which appears at about $519/526\text{ cm}^{-1}$ in PED, was also found to be unresolved for the samples specified in Figure 5. The results quoted above are not dependent on the choice of guest and host isotopes: measurements on a solution-grown mixed crystal mat containing 3% PEH (M_w 50 800) in a PED matrix showed that splitting of the CH_2 bending doublet was unresolved.

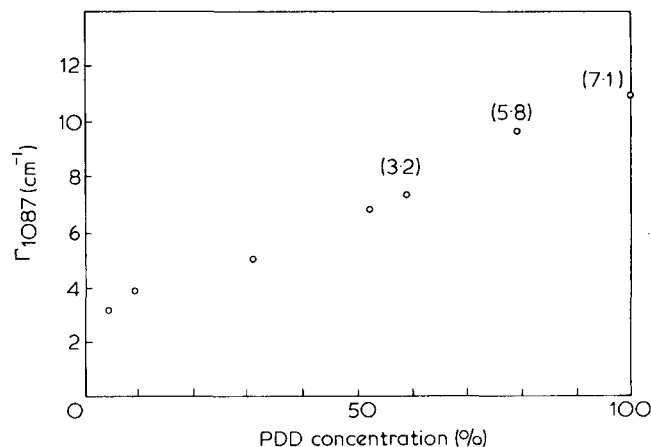


Figure 3 Variation of Γ_{1087} with PDD concentration for mixed paraffin ($\text{C}_{32}\text{H}_{66}$) crystals. Splittings, where resolved, are given in brackets

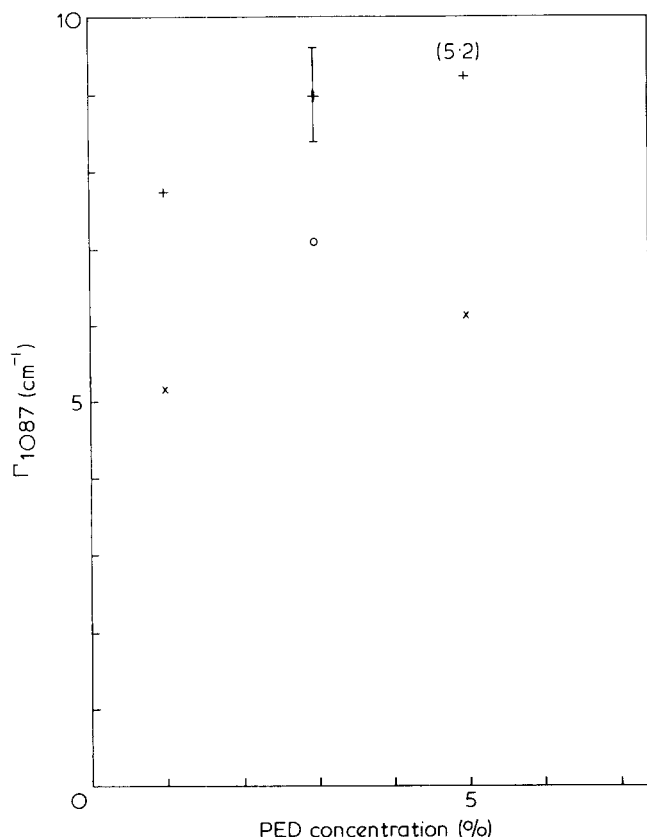


Figure 4 Variation of Γ_{1087} for mixed polyethylene crystals with concentration of PED. The 'guest' PED M_w : +, 386 000; \circ , 103 000; x, 93 000. The resolved splitting is given in brackets

Neutron scattering

The principal aim is to clarify the interpretation of i.r. experiments, and hence the analysis of SANS, described in more detail elsewhere², is summarized with particular emphasis on signals attributable to fractionation according to isotope. In this way we aim to derive a distinction between those i.r. effects which correspond to inter-chain interactions (affected by concentration and fractionation) and those which correspond to intra-chain interactions (related directly to chain conformation).

The values of difference intensities are normalized so that each one is the ratio of the observed count rate to that which would be observed if there were no correlations between the deuterium nuclei in the sample blend. Hence, if all of the deuterium nuclei in one molecule are scattering in phase, the intensity I_o would be given by the number of deuterium atoms per molecule (i.e. molecular weight divided by 8). For $2\pi sR_g < 1$, I can be expressed using:

$$\frac{1}{I} = \frac{1}{I_o} + 4\pi(R_g)^2 s^2 / 3I_o \quad (1)$$

For these systems, the condition $2\pi sR_g < 1$ can in practice be somewhat relaxed (see below). Figure 6 shows an example of a corresponding plot. As described previously by ourselves² and others⁴ the intensity is observed to be higher than expected at the lowest values of s . It has been found^{2,11} that I can be described as a sum of two components: one obeys equation (1) and the other, I_d , obeys equations calculated for two phase structures. It is clear that I_d is associated with some degree of fractionation of one isotopic species with respect to the other. This is

expected if, for example, the PED component crystallizes more slowly than the PEH. It may be noted in passing that Summerfield *et al.*¹¹ interpret the fractionation signal I_d in a slightly different way from ourselves. The difference derives from the scale on which the fractionation is assumed to occur, but a detailed discussion of this is not taken further, other than to remark that our interpretation is consistent with the basic concepts and terminology of Summerfield *et al.* The practical consequence is that the measured intensity can be fitted with either three adjustable parameters² or four¹¹, depending on the choice of function for I_d . This fitting is fairly straightforward in the present case since R_g is rather small. Hence equation (1) describes a more slowly varying function of s compared with I_d , which decreases approximately as s^{-4} . The signal from dispersed molecules is derived in practice by fitting a straight line at larger s (Figure 6(a)) and I_d is obtained at smaller s as the difference between the measured and extrapolated intensities. I_d is then plotted separately (see Figure 6(b) in this work and Figure 4 of ref. 2). The condition that $2\pi sR_g$ should be less than one for the use of equation (1) is fulfilled when I_d is small (this applies to about half the samples shown in Table 1, which includes all those used in ref. 12). When I_d is larger (e.g. as in Figure 6), the maximum value of $2\pi sR_g$ is about 2. These results give comparable values for I_o and R_g , so we conclude that the scattering obeys equation (1) even when $2\pi sR_g$ exceeds unity. The information now available is I_o (which is compared with the molecular weight as a check on consistency), R_g , and a quantity related to the degree of fractionation $(\Delta\rho)^2 A$. $\Delta\rho$ is proportional to the scattering length density difference between the zones enriched and depleted in PED. With the present units of I , $\Delta\rho$ is expressed as number of deuterium atoms per \AA^3 . A is the ratio of the surface between the zones to the total volume. This analysis involves the simplification that only two density values exist. In fact the density will vary continuously over the sample. If we assume that A will be similar for samples crystallized under very similar conditions, the value of $(\Delta\rho)^2 A$ will vary with total PED concentration in a way which will depend on $\Delta\rho$, and hence on the mode of fractionation. If, for example, the enriched zone was of constant volume, $\Delta\rho$ would be

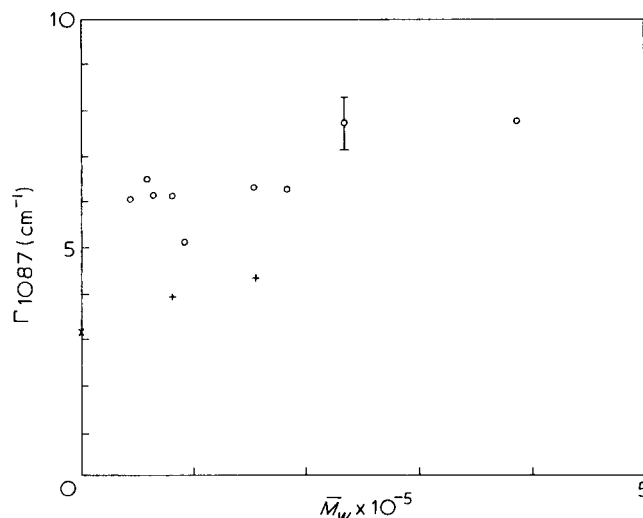


Figure 5 Variation of Γ_{1087} with molecular weight for mixed polyethylene crystals grown from solution with \circ , 1% PED; x, 3% PDD; +, Mats with 1% PED, quenched from the melt. No doublets were resolved

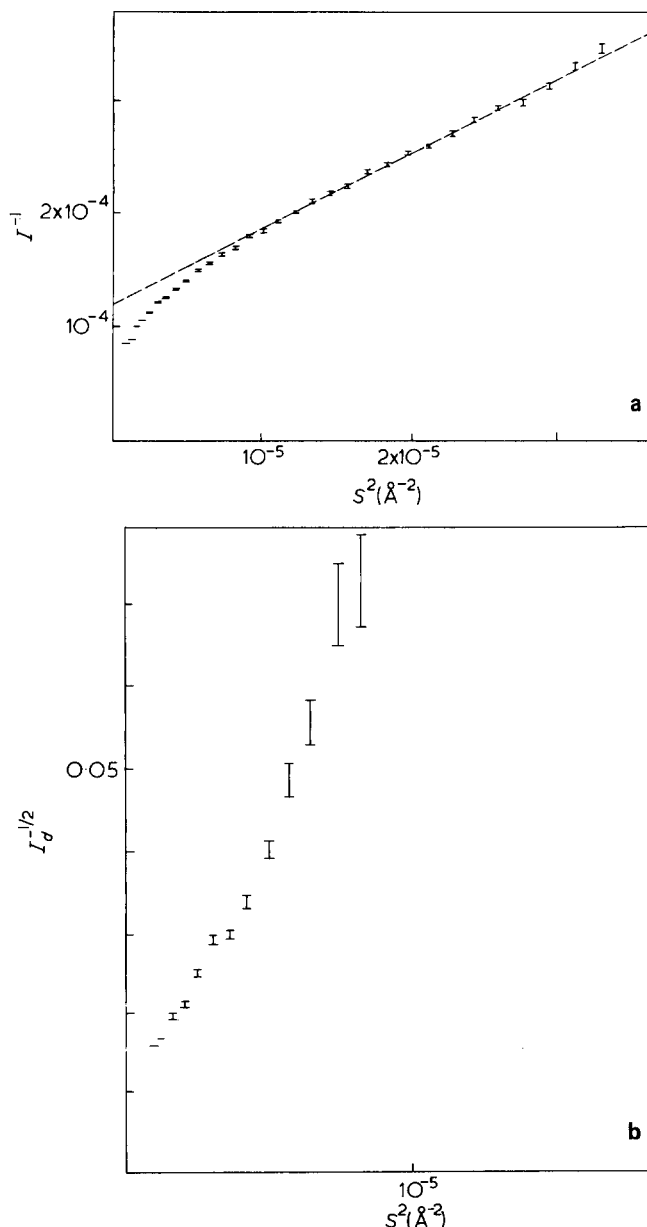


Figure 6 (a) Zimm plot for a mixed polyethylene mat, containing 3% PED of $M_w = 198\,000$ and crystallized from xylene at 70°C . The solid line shows the extrapolation to very small angles for dispersed molecules. (b) I_d , the difference between the extrapolated and observed intensities in (a) is plotted here in the form of $I_d^{-1/2}$ versus s^2 . Unlike other cases, $2\pi s R_g$ exceeds unity. This is discussed in the text

expected to be proportional to the overall PED concentration. It has been estimated² that for an overall PED concentration of 1.4%, $\Delta\rho$ corresponds, very approximately, to 3%.

The measurements of $(\Delta\rho)^2 A$ give an estimate of the maximum probable local concentrations of PED within the samples concerned. From *Table 1* we see that, as expected, $\Delta\rho$ increases with concentration; however, it also increases with molecular weight. This latter observation might be considered surprising in that the supercooling corresponding to a given crystallization temperature increases slightly with molecular weight, and as a rule crystallization rates increase with supercooling. If this were the case, the PED (which has lower melting and dissolution points than PEH) would co-crystallize more intimately with PEH for higher molecular weight, in which case the difference in supercooling for the same crystallization temperature becomes smaller. There is,

however, an explanation for this apparent anomaly: we know that the rate of crystallization decreases with molecular weight for sufficiently long molecules, because of kinetic, rather than strictly thermodynamic reasons, as is well documented¹⁸. In order to interpret the i.r. results, it must be borne in mind that fractionation still occurs, although to a minimal extent, at high supercoolings and that the maximum local isotopic concentration increases with molecular weight.

We note that the molecular weight of PEH also influences the fractionation (see *Table 1*). It may be inferred that the lower molecular weight PEH has a slower crystallization rate, and hence the discrepancy between crystallization rates for PEH and PED becomes less.

DISCUSSION

The main conclusions from earlier neutron scattering studies have already been quoted in the Introduction. As they are basic for the argument to follow, they will be restated. A given chain forms a sheet-shaped object, the thickness of which, up to $\sim M_w/50\,000$, corresponds closely to that expected from a single row of stems. For higher molecular weights the sheets become thicker, while R_g remains practically unchanged. These two effects, individually and in combination, lead to the newly-recognized feature of superfolding. A schematic representation of such superfolded chains is shown in *Figure 7(a)*. The i.r. results will now be considered in this light.

First, the concentration dependence of Γ for polyethylene mixed crystals (*Figure 4*) may be compared with equivalent data for paraffin mixed crystals (*Figure 3*). As was noted at the beginning of the Results section, a PDD concentration of about 55–60% is required for the CD_2 bending doublet to be resolved for mixed paraffin crystals, whereas for mixed polyethylene crystals a PED

Table 1 The fractionation parameter $(\Delta\rho)^2 A$ obtained for solution grown crystals from SANS measurements with $s < 0.01\ \text{\AA}^{-1}$. PED was supplied by Merck, Sharp and Dohme and fractions were made in two ways: (1)* obtained in small quantities using an analytical g.p.c. These molecular weight values are estimated peak molecular weights by g.p.c. G.p.c. analysis of such samples indicates a ratio M_w/M_n of about 1.5. (2) Other PED fractions were obtained by fractional crystallization and liquid-liquid separation and M_w/M_n ratios were in the range between 1.6 and 2.2 (M_n is the number average). The PEH was unfractionated in the cases where $M_w = 109\,000$, otherwise M_w/M_n was approximately 2. +, Samples grown so as to enhance the fractionation (see text — sample type 2(c))

Molecular weight of PED $\times 10^3$ (M_w)	Weight fraction of PED $\times 10^2$	Molecular weight of PEH $\times 10^{-3}$ (M_w)	Crystallization temperature ($^\circ\text{C}$)	$(\Delta\rho)^2 A \times 10^{10}\ \text{\AA}^{-7}$
59	0.6	7	70	4
59	1	7	70	56
59	10	7	70	762
39*	1.4	109	70	1.4
39*	1.4	109	85	220
155	1	42	70	12.2
93	1	42	70	9.8
183	1	42	70	18.7
234	1	42	70	
197.7	1	110	70	55.2
197.7	3	110	70	162
103	1	110	70	59
64.5	1	110	70	25.3
45.7	1	42	70	3.3
207	10	109	70 ⁺	1900
59	1	109	1 ^o /min cooling	36 000

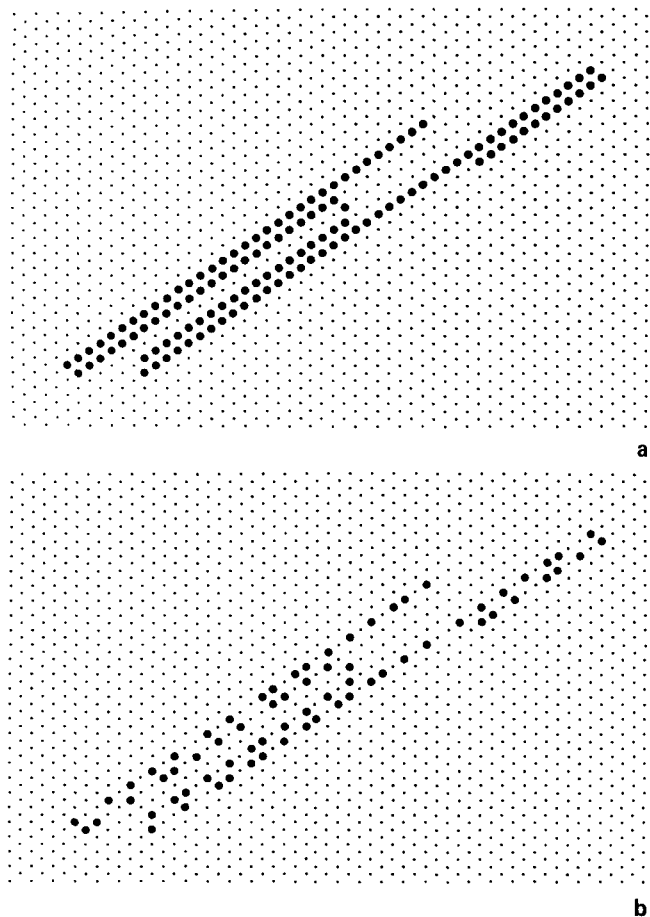


Figure 7 Schematic representation of 'stem' positions of two labelled molecules (large dots) as viewed in the chain direction (i.e. $\{001\}$). The $\{100\}$ direction is shown horizontal, and the fold plane is $\{110\}$ ¹⁹. (a) Strictly adjacent re-entry, (this diagram is adopted from Fig. 2 of ref. 12). (b) Reduced fraction of stems along each sheet which belong to the same molecule

concentration of only 5% is required for resolution of the doublet. Even at PED concentrations of 1% (Figure 5), where the degree of isotopic fractionation as judged from SANS measurements (Table 1) is small, typical values of Γ are much larger than those observed for mixed paraffin crystals with similar guest concentrations. We conclude therefore that polyethylene crystallizes from solution so that the stems are in a much more compact form than guest paraffin chains.

Before proceeding further we have to distinguish between two sources of stem-stem interaction responsible for band broadening, namely intra-molecular and inter-molecular. The former is associated with the conformation of the chain, the latter with the environment of a chain as a whole. That interchain effects do exist is revealed by the observation that the band profiles are affected by concentration, as is clearly shown in the range of 3–5% PED content. Thus, for example, doublets can in some cases be resolved at 5% concentration, but not at 3 or 1%. Bank and Krimm also observe variations of peak profiles (increased splittings with concentration) at guest concentrations of ~5% and higher⁵. Clearly, inter-molecular effects imply close proximity of PED chains. By calculating a quantity analogous to the parameter c^* , familiar in the context of solutions (c^* =critical solute concentration), we find that for the R_g values in question, the PED molecules ought to be well apart on average, even at guest concentrations as high as 3%. The

finite concentration effect in this range presumably arises because the local concentration can be increased by the fractionation, which is revealed by our SANS measurements (Table 1). Clearly our primary interest lies in the conformational effects. The influence of intermolecular effects can be assessed from Figure 4. It is reassuring to note by comparison of the relevant data points in Figure 4 and Figure 5 that differences in morphologies have a much larger effect on the band profiles than differences in concentration, at least within the concentration range in question. Thus, the largest part of the variations in Γ must be due to conformational changes, the guest stems being more randomly arranged for crystallization by quenching from the melt than for solution crystallization. Such a difference could not arise from fractionation effects alone as, according to the SANS technique, variations in local concentrations due to fractionation are shown to be of similar magnitude (1–5%) to the variation in total concentration featuring in Figure 4. Thus the influence of fractionation can only be a minor one and will not mask the effects due to conformational differences. The band profiles at the lowest concentration used (1%) are expected to reflect chain conformational effects to the largest extent and are hence most informative for the present purpose.

However, it follows that interpretation of small differences in Γ requires circumspection, as here the distinction between intra- and inter-molecular effects is not clear-cut. Thus the small increase in Γ with M_w (Figure 5) may well be consistent with superfolding (increased intra-molecular stem-stem interaction): nevertheless, since our SANS results (Table 1) show that fractionation also increases with molecular weight, this cannot be asserted with full confidence from the band profile data above. It is the near invariance of R_g with molecular weight variation which thus remains the primary evidence for superfolding.

In what follows we may attempt to estimate the local stem concentration due to a given molecule. Without a reliable theoretical basis this is purely empirical: nevertheless, in view of the emerging unexpected correlation between the two entirely different techniques, this may merit attention.

We shall make the assumption that on the scale of the intra-chain interactions which contribute to the i.r. peak broadening, the spatial arrangements of labelled stems in mixed paraffin and mixed polymer systems with similar overall guest concentrations differ only in terms of the local concentration of these stems. This implies that on a local scale there is no preferred crystallographic direction for the positions of labelled stems in mixed polymer crystals. The latter cannot be strictly true, as we have seen from SANS measurements in the scattering range $10^{-1} > s > 10^{-2} \text{ \AA}^{-1}$ that the stems lie along preferential fold planes (from the overall sheet-like nature of the scattering entity), not to speak of all the earlier evidence of sectorization in favour of preferential fold planes. Nevertheless, at molecular weights sufficiently high for superfolding to be well developed, stems from a given guest chain will have increasingly large numbers of neighbours in directions other than the fold plane. Hence at least on the local scale, the above condition, namely the absence of a preferred crystallographic arrangement of guest neighbours, is gradually approached. Thus we may now apply the criterion of taking equal Γ values in polymers and paraffins and use the appropriate concentration value

for the paraffin system to define the local stem environment in the chain folded polymer. In the latter case, the average stem concentration for a given folded molecule would be in the range of 45–65%. If we now refer to the particular fold plane, then this figure corresponds to the stem occupancy due to a given molecule along a chain folded ribbon. This would mean that the stem re-entry is not completely adjacent but that 35–55% of the stems along a given sheet are not parts of the same molecule.

The relevant parameter in the SANS result is n_A which is proportional to the occupation density for labelled chains along the sheet². As noted in the Introduction this does not correspond to exclusive occupancy by labelled chains, but is lower by a factor of approximately two. This departure from predictions from strictly adjacent re-entry, while reported, was not discussed specifically at that time. Nevertheless, in view of its systematic recurrence, it is likely to have a real structural basis, in which case it would mean dilution of the labelled stems with stems from other (matrix) molecules. As we have seen above, this is just the inference which was made by comparing i.r. band shapes from the polymer and paraffin spectra, a method which led to broadly similar numerical values. The above discussion leads to the model described schematically in Figure 7(b). It may be asked why the stem density along the growth front should be half that for adjacent re-entry. This could be because molecules do not crystallize singly on the growth face, but rather that there is a concentrated strip of solution along the crystal edge¹⁸. This would lead not only to the 'competition' between chains which we suppose leads to superfolding¹², but also to intermixing between co-crystallizing molecules. The precise way in which the intermixing occurs will be considered in a further publication.

CONCLUSIONS

The i.r. measurements presented here lend support to the model derived from SANS measurements for chain folding in solution-grown polyethylene. In this model, individual chains fold along a specific plane to form sheet structures. For molecular weights above about 50 000 the chain-folded ribbons fold back upon themselves ('superfolding') and this behaviour is believed to be responsible for the insensitivity of R_g to change in molecular weight.

A comparison of the dependence of Γ on guest concentration for solution-grown polyethylene and mixed paraffin crystals confirms that the polymer molecules have a compact conformation, although the detail of the peak profile is affected by inter-chain effects, at least with a guest concentration of 3%. Estimates of the degree of isotopic fractionation in mixed polyethylene samples by SANS show that fractionation effects are probably negligible for PED concentrations of 1%. The increase in Γ with increasing PED molecular weight for mixed polyethylene crystals containing 1% PED may be partly due to an increase in the degree of isotopic fractionation with increasing molecular weight, but this behaviour is probably superimposed on a conformational effect: in the case of superfolded chains, the number of interactions between CD₂ groups would increase continually with increasing chain length.

Finally, we make the suggestion that typical values of the i.r. bandwidth parameter Γ for solution grown mixed paraffin and mixed polyethylene crystals and of the area density of labelled nuclei, derived from SANS, both indicate a dilution of stem site occupancy along the fold

plane due to one and the same chain. By both measurements the fraction of lattice stem sites occupied by a given molecule appears to be closer to 0.5 than to unit.

NOTE ADDED IN PROOF

We wish to note here that the infra-red measurements have been repeated using a Nicolet 7000 series Fourier Transform Interferometer and samples cooled to liquid nitrogen temperatures. Although the conclusions from this work are not fundamentally changed, we wish to draw attention to several features which have emerged from the later work. The reduced lattice dimensions at lower temperatures, and the improved signal-to-noise ratio of the interferometer for weak absorption bands (compared with dispersive instruments) have led to the observation of a multiplet band structure, where previously only a broad single peak was observed. We now recognize that the distinction drawn above (see Results) between samples which produce a resolvable doublet splitting and those which do not is somewhat arbitrary, since it depends on characteristics of the spectrometer used and on the sample temperature. However, the trends in i.r. parameters with those variables used here are generally confirmed. Moreover, the ability to measure peak separations rather than relying on overall bandwidths has increased the precision of our measurements and enabled us to study more dilute systems. From peak separations measured for polymer and paraffin systems, we now obtain a figure of 50–80% as the average polymer stem concentration for a single molecule along the fold plane, for an overall PED concentration of 0.5%. The molecular weight dependence of band splitting (Figure 5) is found to be larger than the concentration dependence (Figure 4), confirming the importance of intra-molecular effects in the molecular weight dependence.

ACKNOWLEDGEMENTS

We would like to thank the Science Research Council for support for one of us (S.J.S.) during the course of this work. We are indebted to the Staff of the Institut Laue Langevin (Grenoble) for assistance with neutron scattering measurements. We would also like to thank Mrs A. Halter for technical assistance in sample preparation and characterization.

REFERENCES

- Sadler, D. M. and Keller, A. *Polymer* 1976, **17**, 37
- Sadler, D. M. and Keller, A. *Macromolecules* 1977, **10**, 1128
- Schelten, J., Wignall, G. D. and Ballard, D. G. H. *Polymer* 1974, **15**, 682
- Schelten, J., Ballard, D. G. H., Wignall, G. D., Longman, C. and Schmatz, W. *Polymer* 1976, **17**, 751
- Bank, M. I. and Krimm, S. *J. Polym. Sci. (A-2)* 1969, **7**, 1785
- Bank, M. I. and Krimm, S. *J. Polym. Sci. (B)* 1970, **8**, 143
- Krimm, S. and Ching, J. H. C. *Macromolecules* 1972, **5**, 209
- Ching, J. H. C. and Krimm, S. *J. Appl. Phys.* 1975, **46**, 4181
- Ching, J. H. C. and Krimm, S. *Macromolecules* 1975, **8**, 894
- Tasumi, M. and Krimm, S. *J. Polym. Sci. (A-2)* 1968, **6**, 995
- Summerfield, G. C., King, J. S. and Ullmann, R. *Macromolecules* 1978, **11**, 218
- Sadler, D. M. and Keller, A. *Science* 1979, **203**, 263
- Hoffman, J. D., Frolen, L. J., Ross, G. S. and Lauritzen, J. I. J. *Nat. Bur. Stds.*, 1975, **79A**, 671
- Frank, F. C. and Tosi, M. *Proc. R. Soc.* 1961, **A263**, 323
- Krimm, S., Liang, C. Y. and Sutherland, G. B. B. M. *J. Chem. Phys.* 1956, **25**, 549
- Schmatz, W., Springer, T., Schelten, J. and Ibel, K. *J. Appl. Crystallogr.* 1974, **7**, 96
- Jacrot, B. *Rep. Prog. Phys.* 1976, **39**, 911
- Keller, A. and Pedemonte, E. *J. Crystal Growth*, 1973, **18**, 111